ACS OMEGA

Open Access

http://pubs.acs.org/journal/acsodf

Article

Enhancement of Sensitivity in Aggregation-Based Whole-Cell Arsenite Sensor Utilizing Arsenic Metabolism Regulation

Shiryu Abe,[⊥] Rina Ayuba,[⊥] Kyohei Ouchi, Yu-ki Tanaka, Ai Fujimoto, Akira Kitamura, Yasumitsu Ogra, Yuki Kimura, Daisuke Umeno, and Shigeko Kawai-Noma*

Cite This: *ACS Omega* 2025, 10, 14199−14208

Read Online

ACCESS | Metrics & More | Article Recommendations | Supporting Information

ABSTRACT: Arsenite [As(III)] is a toxic substance widely present on Earth, and the development of low-cost and simple microbial-based As(III) sensors has been attracting attention. Recently, we discovered that the protein LuxR, which contains multiple cysteine residues with high affinity for As(III), forms an insoluble structure upon binding to As(III) and exhibits OFF-switching properties as a quorum sensing transcriptional activator. Based on this property, the LuxR sensor operates on a new principle distinct from conventional whole-cell As(III) sensors; however, its sensitivity remains a challenge. In this study, we aimed to improve the sensitivity of the whole-cell OFF-type As(III) sensor by increasing the frequency of intracellular interactions between the sensor protein and As(III). We utilized the super-repressor properties of ArsR, a transcriptional repressor of the As(III)-metabolizing *ars* operon, achieved by replacing C34 in its As(III)-binding domain with Y. By linking $ArsR_{C34Y}$ with the OFF-type As(III) sensor protein LuxR, we constructed a single plasmid to create a portable $ArsR_{C34Y}$-LuxR sensor protein. By suppressing the expression of ArsB, an As(III) efflux transporter encoded in the *ars* operon, using $ArsR_{C34Y}$, we successfully enhanced the sensitivity of the OFF-type As(III) response.

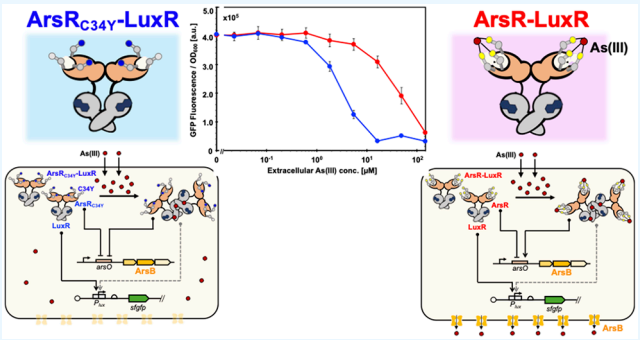

INTRODUCTION

Arsenite [As(III)] is toxic, but its toxicity varies depending on its chemical form, with inorganic As(III) being particularly harmful. As(III) naturally exists in various parts of the world, and it has been reported that over 140 million people drink arsenic-contaminated water daily.[1] Long-term exposure to As(III) leads to arsenicosis, various skin diseases, and cancer. The World Health Organization (WHO) has set a safety standard for As(III) concentration at 10 ppb (133.5 nM), making it extremely important to monitor and detect As(III) in the environment.[2] Traditionally, when investigating As(III) contamination in the environment, expensive analytical instruments such as atomic absorption spectroscopy (AAS), gas chromatography−mass spectrometry (GC−MS), and inductively coupled plasma−mass spectrometry (ICP−MS) are commonly used for As(III) detection.[3−5] These devices are highly sensitive, but their high cost and the specialized expertise required for operation and analysis limit their general applicability.

Recently, whole-cell biosensors have been developed for detecting environmental contaminants due to their robustness, eco-friendliness, and cost-effectiveness.[6−9] In contrast to traditional physical and chemical sensors, cellular sensors are renewable, highly selective, easy to manufacture, and cost-efficient.[10,11] Whole-cell sensors that utilize the As(III) metabolism *ars* system in bacteria have been developed for As(III) detection. In this system, the transcriptional repressor ArsR, which regulates the expression of the *ars* operon, binds to As(III), causing it to dissociate from the operator sequence pArs, thereby lifting transcriptional repression.[12−14] By placing visually detectable reporters like *β*-galactosidase or GFP genes downstream of pArs, this sensor system enables As(III) detection.[15−20] As(III) is known to have a high binding affinity with the thiol groups of cystein.[21,22] ArsR contains an As(III)-binding domain with three cysteine residues (C32, C34, and C37), and when As(III) binds to these cysteines, ArsR undergoes a significant conformational change, dissociating from pArs to lift transcriptional repression.[21,23,24] Using this system for whole-cell sensors has been common due to its established methodology.

We recently discovered that LuxR, a quorum-sensing regulator in *Vibrio* species with multiple cysteines,[25−27] aggregates in response to As(III), switching its function even

Received: December 30, 2024
Revised: March 24, 2025
Accepted: March 25, 2025
Published: April 3, 2025

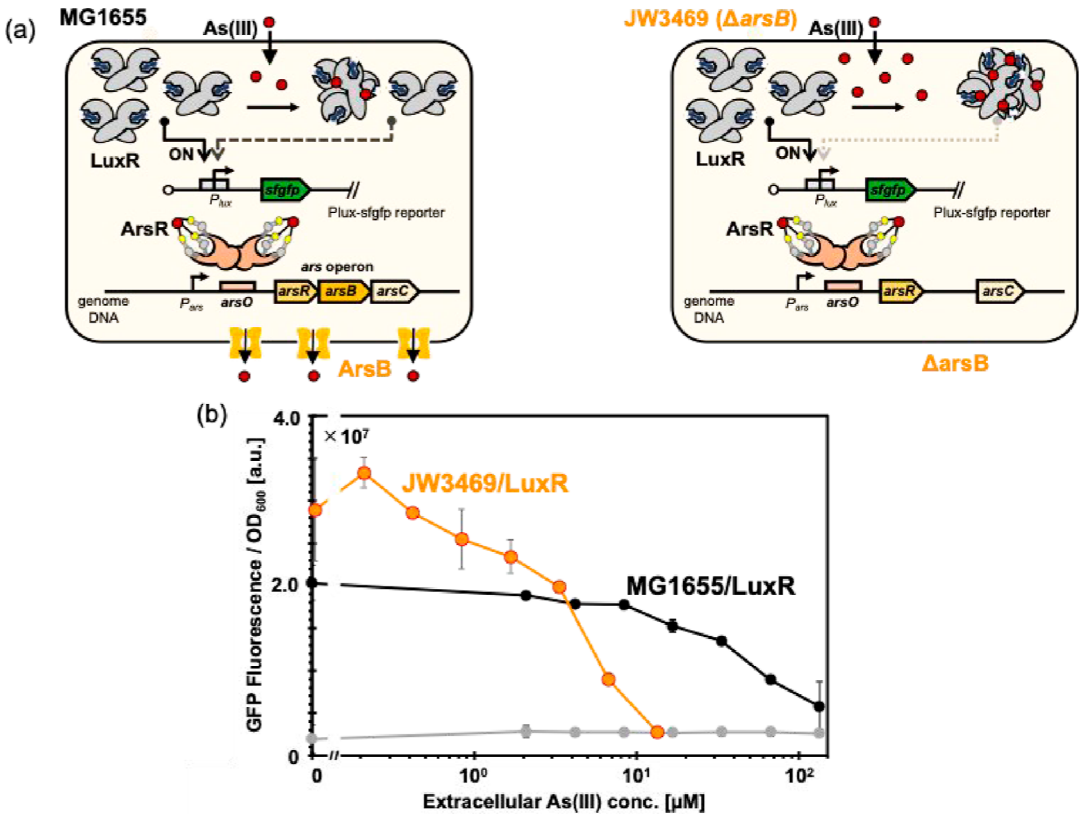

Figure 1. Enhanced sensitivity of LuxR sensor to arsenite (As(III)) in the ArsB-deficient mutant strain. (a) Schematic model of LuxR aggregation-induced transcriptional OFF-switch in response to intracellular As(III) levels. LuxR is a transcriptional activator of the *lux* promoter (pLux) in response to its ligand, AHL (indicated as blue molecules bound to LuxR). AHL acts as a quorum signal to activate the reporter gene (*sfgfp*) expression under pLux regulation. ArsR is a transcriptional repressor that regulates the expression of the *ars* operon by binding to the *ars* operator (*arsO*). Upon As(III) binding (red circles) to the cysteine residues (C32, C34, and C37; highlighted in yellow) in ArsR, the repressor dissociates from *arsO*, allowing expression of the *ars* operon. The *ars* operon encodes ArsB, a membrane protein responsible for As(III) efflux. In the wild-type MG1655 strain (left), ArsB expression facilitates As(III) metabolism, whereas in the *arsB*-deficient JW3469 strain (right), As(III) metabolism is impaired, leading to enhanced sensitivity. (b) Dose-dependent response of LuxR to As(III). Black circles indicate MG1655 strains expressing the LuxR sensor; yellow circles indicate JW3469 strains expressing the LuxR sensor; and gray circles indicate MG1655 strains expressing only the vector. The cultured cells were collected after 12 h treated with 10 μM AHL and appropriate As(III) concentrations. Each data point represents the average of three independent experiments, with error bars showing standard deviations.

though it has no direct functional relationship with As(III) metabolism.[28] We reported that this phenomenon could be used to develop a novel whole-cell sensor with a completely different operational principle than conventional ones. LuxR has nine cysteines, which cause aggregation when the As(III) concentration in the medium exceeds 133.5 μM, resulting in the loss of transcriptional activation function of LuxR and a functional switch due to aggregation.[28]

Although this As(III)-induced LuxR aggregation-based functional switch sensor had a novel operational principle distinct from conventional As(III)-induced ArsR conformational change sensors, it was limited by its high response threshold of 133.5 μM for extracellular As(III) concentration. To address this limitation, LuxR aggregation must be triggered at a lower extracellular As(III) concentration than 133.5 μM. By effectively promoting the binding reaction between As(III) and LuxR within the cell, it is possible to achieve LuxR aggregation and functional switching at even lower extracellular As(III) concentrations, thereby enhancing the sensitivity of the As(III) sensor.

In this study, we developed a novel whole-cell As(III) sensor with high sensitivity to lower concentrations of As(III) by suppressing the expression of the As(III) exporter ArsB encoded in the *ars* operon using a super-repressor mutant $ArsR_{C34Y}$. This report further investigates the factors that contributed to this enhanced sensitivity and identifies cellular conditions that effectively promote the reaction between the sensor protein and As(III).

RESULTS AND DISCUSSION

Sensitivity Enhancement of the LuxR Sensor through an arsB-Deficient Strain. ArsB, which promotes As(III) efflux in *Escherichia coli*, is encoded in the As(III) metabolism-related *ars* operon, and its expression is regulated by ArsR.[29] We hypothesized that by constantly suppressing the expression of ArsB to inhibit the efflux of As(III) taken up by the cells, it would be possible to enhance the sensitivity of the LuxR-based whole-cell As(III) sensor we have already developed (Figure 1a). To test this, we expressed LuxR in the *arsB*-deficient strain JW3469 from the KEIO collection[30] and measured its response to As(III) added to the medium by placing superfolder green fluorescent protein (sfGFP) downstream of pLux and monitoring fluorescence intensity.

Compared to the wild-type MG1655 strain, which harboring ArsB, the sensitivity of the whole-cell As(III) sensor was enhanced, showing an OFF-type As(III) response curve with a

https://doi.org/10.1021/acsomega.4c11704
ACS Omega 2025, 10, 14199−14208

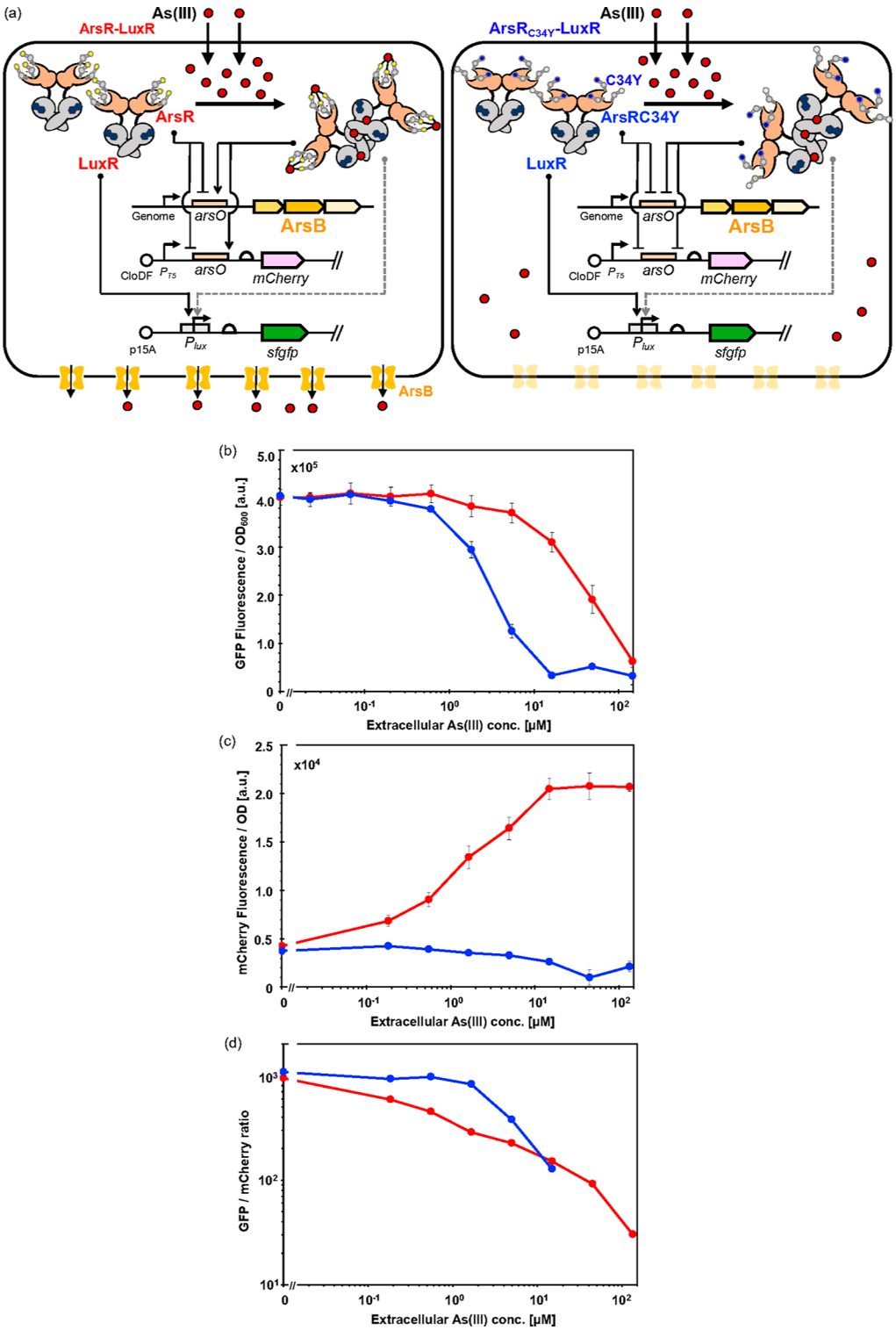

Figure 2. Response of ArsR-fused LuxR sensors to As(III). (a) Model of intracellular arsenic metabolism regulation by ArsR-LuxR and $ArsR_{C34Y}$-LuxR. In MG1655 strains expressing ArsR-LuxR (left), the ArsR bound to As(III) induces the expression of ArsB encoded in the *ars* operon, allowing As(III) to be metabolized. In contrast, in MG1655 strains expressing $ArsR_{C34Y}$-LuxR with the C34Y mutation (right), the super-repressor activity of $ArsR_{C34Y}$ prevents operon expression, inhibiting As(III) efflux by ArsB. (b) Dose-dependent response to As(III) of ArsR-LuxR and $ArsR_{C34Y}$-LuxR. MG1655 strains expressing ArsR-LuxR sensors (red circles) and those expressing $ArsR_{C34Y}$-LuxR sensors (blue circles) were analyzed. Each strain was cotransformed with the reporter plasmids pLux-sfgfp (to evaluate the As(III)-dependent transcriptional activation by LuxR) and pArs-mCherry (to assess the As(III)-dependent transcriptional repression by ArsR or $ArsR_{C34Y}$). sfGFP fluorescence induced by pLux-sfgfp is shown. Each plot represents the average of three independent experiments, and error bars indicate standard deviations. (c) Dose-dependent response to As(III) of ArsR-LuxR (red) and $ArsR_{C34Y}$-LuxR (blue). mCherry fluorescence induced by pArs-mCherry is shown. Each plot represents the average of three independent experiments, and error bars indicate standard deviations. (d) The GFP/mCherry ratio as a function of extracellular As(III) concentration in strains expressing ArsR-LuxR (red) and $ArsR_{C34Y}$-LuxR (blue).

https://doi.org/10.1021/acsomega.4c11704
ACS Omega 2025, 10, 14199−14208

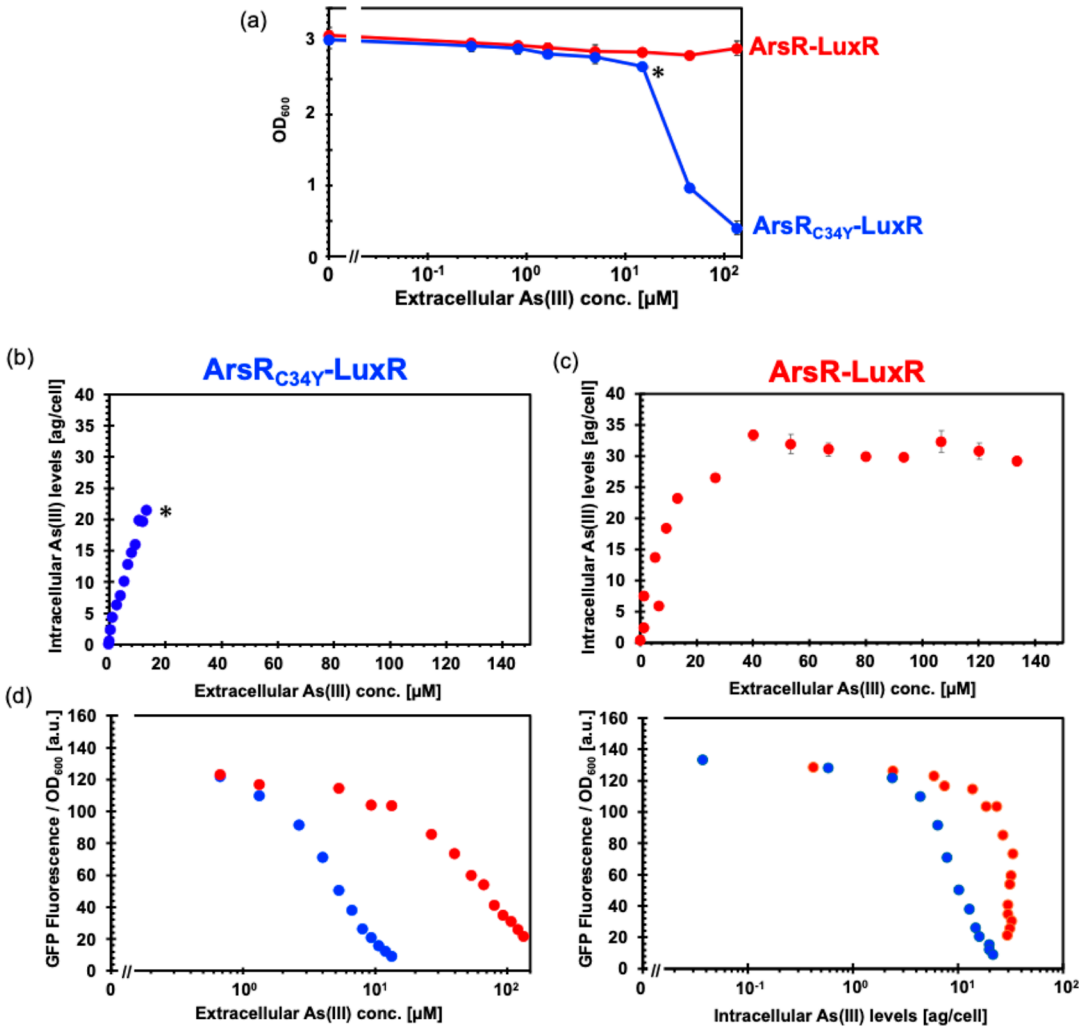

Figure 3. Intracellular As(III) levels in response to extracellular As(III) concentrations for ArsR$_{C34Y}$-LuxR in MG1655 and ArsR-LuxR in MG1655. (a) OD$_{600}$ dose-responsive changes to As(III). The colors of the plots correspond to those in Figure 2. Asterisk (*) indicates the point at which growth inhibition in ArsR$_{C34Y}$-LuxR strain. Each plot represents the average of three independent experiments, and error bars indicate standard deviations. (b) Intracellular As(III) levels of ArsR$_{C34Y}$-LuxR in MG1655 as a function of extracellular As(III) concentration, measured by ICP−MS. Each plot represents the average of three independent experiments, and error bars indicate standard deviations. (c) Intracellular As(III) levels of ArsR-LuxR in MG1655 as a function of extracellular As(III) concentration, measured by ICP−MS. Each plot represents the average of three independent experiments, and error bars indicate standard deviations. (d) Dose-dependent response to extracellular As(III) for ArsR$_{C34Y}$-LuxR in MG1655 (blue circles) and ArsR-LuxR in MG1655 (red circles) (left panel). The graph (right panel) shows the arsenic response of each strain as intracellular arsenic levels, calculated from the ICP−MS results.

minimum As(III)-responsive fluorescence output value of 5 × 10^6 at a 13.35 μM As(III) concentration, 1 order of magnitude lower (Figure 1b). No decrease in OD$_{600}$ was observed at As(III) concentrations up to 13.35 μM (Figure S1). From these results, it was found that the JW3469 strain lacking ArsB expression was unable to excrete As(III), and, as we expected, the sensitivity of the whole-cell As(III) sensor utilizing LuxR was enhanced. This indicates that the deletion of the As(III) efflux factor ArsB effectively increases the sensitivity of the whole-cell sensor by enhancing the frequency of interactions between the ligand (As(III)) and the sensor protein LuxR.

LuxR Aggregation-Based Functional Switch As(III) Sensor Fused with the As(III) Metabolism Regulator ArsR. To enable high-sensitivity As(III) response using LuxR, which exhibits aggregation properties in the presence of As(III), the *arsB* gene must be knocked out in the genome of each *E. coli* strain. While genome recombination has become simpler, a plasmid expression system that can easily induce the same phenomenon across different strains is very appealing from the perspective of portability of genetic information. We considered recreating the effect of *arsB* deletion by using a plasmid expression system for ArsR, focusing on the super-repressor ability conferred by mutations in the As(III)-binding domain of ArsR (Figure 2a). ArsR has three cysteines (C32, C34, and C37) in its As(III)-binding domain, and studies by Rosen and colleagues have shown that substituting any of these with other amino acids prevents ArsR from dissociating from DNA in the presence of As(III), thereby inhibiting the expression of the *ars* operon.[23] We introduced the C34Y mutation used in their study into ArsR. Additionally, ArsR has three other cysteines that could serve as potential As(III)-induced aggregation linkage points, so we fused LuxR with ArsR$_{C34Y}$, expecting enhanced aggregation due to an increase in linkage points compared to LuxR alone. We constructed an ArsR$_{C34Y}$-LuxR fusion sensor with both As(III) sensing and As(III) metabolism regulatory capabilities.

https://doi.org/10.1021/acsomega.4c11704
ACS Omega 2025, 10, 14199−14208

First, we examined whether ArsR-LuxR, with wild-type ArsR fused, exhibits As(III) response similar to that of LuxR alone, and whether $ArsR_{C34Y}$-LuxR, expected to have super-repressor activity, shows an As(III) response similar to that of the *arsB*-deficient strain (Figure 1b). We introduced both the sensor plasmid and reporter plasmids with sfGFP placed downstream of pLux and with mCherry placed downstream of pArs into the MG1655 strain and measured fluorescence intensity. The MG1655 strain expressing the ArsR-LuxR sensor (hereafter referred to as the ArsR-LuxR strain) exhibited an OFF-type output, with fluorescence output reaching its minimum at an extracellular As(III) concentration of 133.5 μM (Figure 2b red). This trend was consistent with that observed for the MG1655 strain expressing the LuxR-only sensor (Figure 1b, black). In contrast, the MG1655 strain expressing the $ArsR_{C34Y}$-LuxR sensor (hereafter referred to as the $ArsR_{C34Y}$-LuxR strain) exhibited an OFF-type output, with fluorescence output reaching its minimum at an extracellular As(III) concentration of 13.35 μM (Figure 2b blue). This trend was similar to that observed for the JW3469 strain expressing LuxR (Figure 1b yellow).

When the transcriptional repression ability of ArsR was evaluated by introducing the pArs-mCherry plasmid as a reporter, mCherry expression was gradually observed from an extracellular As(III) concentration of 0.1335 μM in the ArsR-LuxR strain, reaching a plateau at 13.35 μM, indicating that ArsR dissociated from DNA in response to As(III) (Figure 2c red). On the other hand, no mCherry expression was observed at any As(III) concentration in the $ArsR_{C34Y}$-LuxR strain, indicating that $ArsR_{C34Y}$ did not dissociate from DNA (Figure 2c blue). These results strongly suggest that $ArsR_{C34Y}$ acts as a super-repressor, suppressing the expression of operons, including *arsB*.

To evaluate the sensitivity differences between ArsR-LuxR strain and $ArsR_{C34Y}$-LuxR strain, we analyzed the ratio of GFP fluorescence to mCherry fluorescence (GFP/mCherry ratio) as a function of extracellular As(III) concentration. The GFP/mCherry ratio for ArsR-LuxR strain showed a gradual decrease with increasing As(III) concentration, indicating that the sensor operates effectively at higher As(III) levels. In contrast, the GFP/mCherry ratio for $ArsR_{C34Y}$-LuxR strain showed a sharp decline at lower As(III) concentrations, reaching its maximum sensitivity at approximately 13.35 μM. This difference suggests that $ArsR_{C34Y}$ promotes intracellular As(III) accumulation by suppressing ArsB expression, enabling the sensor to respond to lower As(III) concentrations.

By constructing a single plasmid-based expression system combining $ArsR_{C34Y}$ and LuxR, we successfully transformed a different strain, BW25113, into a highly sensitive OFF-type As(III) sensor with ease (Figure S2). This approach enables a straightforward method to enhance the sensitivity of OFF-type As(III) responses without the need to create *arsB*-deficient strains for each host.

Reasons Contributing to the Increased Sensitivity Brought About by the Super-Repressor $ArsR_{C34Y}$. The $ArsR_{C34Y}$-LuxR strain exhibited the minimum As(III)-responsive fluorescence output at an extracellular As(III) concentration of 13.35 μM, which was 1 order of magnitude lower than that of the ArsR-LuxR strain (Figure 2b). To investigate the reason for this phenomenon, we examined it from the perspective of intracellular As(III) concentrations. Specifically, we hypothesized that the suppression of ArsB expression in the $ArsR_{C34Y}$-LuxR strain inhibited the efflux of intracellularly accumulated As(III), thereby enhancing sensitivity. To test this hypothesis, intracellular As(III) concentrations at various extracellular As(III) concentrations were measured using ICP−MS.

In *E. coli* expressing $ArsR_{C34Y}$-LuxR, no significant effect on growth was observed at extracellular As(III) concentrations up to 13.35 μM. However, at concentrations exceeding this threshold, growth inhibition was observed, as evidenced by a decrease in OD_{600} values (indicated by the asterisk in Figure 3a). Within this range, intracellular As(III) levels increased linearly with extracellular As(III) concentration, eventually reaching approximately 20 ag/cell (indicated by the asterisk in Figure 3b). In contrast, the ArsR-LuxR strain showed no growth inhibition at extracellular As(III) concentrations up to 133.5 μM (Figure 3a red). As the extracellular As(III) concentration increased to 133.5 μM, intracellular As(III) levels also increased linearly (Figure 3c). However, as the As(III) concentration increased further, intracellular As(III) levels gradually plateaued at approximately 30−35 ag/cell (Figure 3c).

The results from both strains revealed that the amount of arsenic a single *E. coli* cell can uptake ranges from 20 to 35 ag/cell. For the first time, we successfully provided an empirical measurement of the upper limit of arsenic uptake by *E. coli* cells before reaching the threshold of arsenic toxicity tolerance. Interestingly, despite ArsB expression, the ArsR-LuxR strain exhibited approximately 1.5 times higher As(III) uptake per cell than the $ArsR_{C34Y}$-LuxR strain, where ArsB expression was suppressed. This discrepancy is likely attributable to the C34Y mutation in the As(III)-binding domain of $ArsR_{C34Y}$-LuxR, which inhibits As(III) binding to the ArsR region. Consequently, the intracellular As(III) levels in the $ArsR_{C34Y}$-LuxR strain were lower than those in the ArsR-LuxR strain.

Next, we replotted the response output of each strain at each extracellular As(III) concentration (Figure 3c left) against the intracellular As(III) levels measured by ICP−MS on the horizontal axis (Figure 3c right). The results showed an inflection point around 4 ag/cell in the $ArsR_{C34Y}$-LuxR strain, where the response output to As(III) gradually decreased, showing an OFF-type curve (Figure 3c right, blue). In contrast, the ArsR-LuxR strain showed a sharp decrease in response output when the intracellular As(III) level exceeded 20 ag (Figure 3c right, red). Ultimately, both strains exhibited the minimum response output within the range of 25−30 ag of intracellular As(III) (Figure 3c).

In summary, when plotted against extracellular As(III) concentrations, the As(III) concentration at which each strain exhibited the minimum response output differed by an order of magnitude. However, when the horizontal axis was converted to intracellular As(III) concentrations, the amount of As(III) per cell corresponding to the minimum output was consistent for both strains, at 25−30 ag/cell. Although the shapes of the intracellular As(III) response curves leading to the minimum fluorescence output differed between the two strains, the reason for this difference remains unverified and cannot be addressed at this time. Nonetheless, these results suggest that the upper limit of As(III) uptake per cell is 25−30 ag/cell. The intracellular arsenic concentration obtained in this study, when converted based on the assumption that the volume of a single *E. coli* cell is 1 fL, was found to be 0.334−0.400 mM. This concentration is extremely high compared to the typical concentrations of intracellular ions and metals. Furthermore, the enhanced sensitivity observed in the $ArsR_{C34Y}$-LuxR strain,

https://doi.org/10.1021/acsomega.4c11704
ACS Omega 2025, 10, 14199−14208

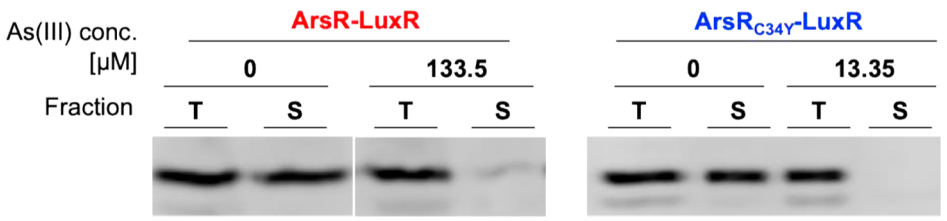

Figure 4. Reduction in the effective concentration of ArsR-LuxR and ArsR$_{C34Y}$-LuxR by As(III). Western blot analysis showed that the band of ArsR-LuxR and ArsR$_{C34Y}$-LuxR in the soluble fraction (S) for the total fraction (T) was reduced at an As(III) concentration of 133.5 or 13.35 μM. The cultured cells were collected after 12 h treated with 10 μM AHL and appropriate As(III) concentrations. After cell lysis, the lysates were separated by 10% SDS-PAGE, and ArsR-LuxR and ArsR$_{C34Y}$-LuxR were detected using a 6× His mAb-HRP conjugate.

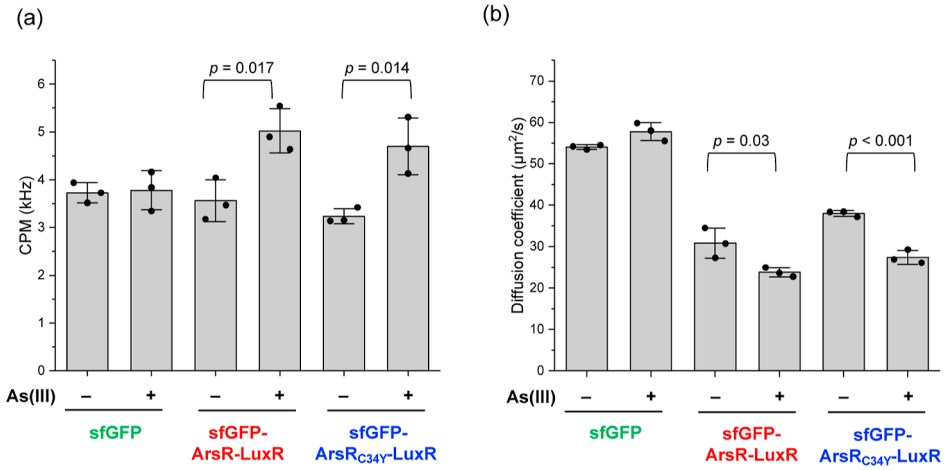

Figure 5. As(III)-dependent aggregation of the sensor ArsR-LuxR and ArsR$_{C34Y}$-LuxR proteins. Fluorescence correlation spectroscopy (FCS) analysis of sfGFP fused ArsR-LuxR, ArsR$_{C34Y}$-LuxR, and sfGFP monomers in the supernatants of lysates. sfGFP monomers were used as a control that does not respond to As(III). (a) Counts per molecule (CPM) of sfGFP-ArsR-LuxR, sfGFP-ArsR$_{C34Y}$-LuxR, and sfGFP. CPM values were normalized to those of sfGFP monomers. (b) Diffusion coefficients of sfGFP-ArsR-LuxR, sfGFP-ArsR$_{C34Y}$-LuxR, and sfGFP. For diffusion coefficients, a single-component analysis was performed for GFP monomers, while a two-component analysis was conducted for other samples, followed by the calculation of the weighted average. The three plots above each bar in (a,b) represent the results of three independent experiments.

which is unable to excrete As(III), is considered to be due to reaching this upper limit at an extracellular As(III) concentration of 13.35 μM.

Molecular State of Both Sensor Proteins in the Presence of As(III). The LuxR sensor we previously reported was an insoluble-type sensor, in which more than half of the expressed LuxR protein precipitated by reacting with As(III) under conditions of 133.5 μM As(III) concentration.[28] Since the ArsR-LuxR and the enhanced-sensitivity ArsR$_{C34Y}$-LuxR developed in this study also showed OFF As(III) response outputs at 133.5 and 13.35 μM As(III) concentrations, respectively, it is expected that these molecules exhibit aggregation-type behavior. We investigated the molecular states of both sensor proteins at each As(III) concentration by Western blotting (Figure 4).

After culturing *E. coli* in the presence of As(III), the cells were lysed. The lysate was centrifuged to separate it into a supernatant fraction and a pellet fraction. The lysate before centrifugation was designated as the total fraction. Each fraction—the total fraction and the supernatant fraction after centrifugation—was analyzed by SDS-PAGE, and the sensor protein in each fraction was detected by Western blot using an anti-His tag antibody. As a result, both ArsR-LuxR and ArsR$_{C34Y}$-LuxR showed nearly identical band intensities in the total fraction and supernatant fraction under As(III)-free conditions, indicating that all expressed proteins were present as soluble proteins. In contrast, under As(III)-added conditions of 133.5 and 13.35 μM, the amount of soluble protein in both sensor proteins decreased relative to the total fraction (Figure 4).

Next, we demonstrated the aggregation of LuxR in response to As(III) using fluorescence correlation spectroscopy (FCS), which detects aggregates through changing the fluorescent brightness in addition to the diffusion coefficient of fluorescent molecules.[31−34] The FCS results were evaluated based on two values: counts per molecule (CPM) and the diffusion coefficient. Since CPM represents the brightness of fluorescent single particles, it directly shows the aggregates. First, the sfGFP monomers showed no significant difference in CPM values between As(III)-added and nonadded conditions (Figure 5a). Next, in As(III)-free conditions, both sfGFP-ArsR-LuxR and sfGFP-ArsR$_{C34Y}$-LuxR showed the same CPM values as the sfGFP monomers, suggesting that they exist as monomers. However, upon As(III) addition, the CPM for both sfGFP-ArsR-LuxR and sfGFP-ArsR$_{C34Y}$-LuxR increased by approximately 1.4 times (Figure 5a). Next, the diffusion coefficient of sfGFP monomers was 55 and 60 μm^2/s, regardless of As(III) addition, as a negative control. With As(III) addition, the diffusion coefficient decreased to approximately 0.4 times for sfGFP-ArsR-LuxR (24 μm^2/s) and approximately 0.5 times for sfGFP-ArsR$_{C34Y}$-LuxR (27 μm^2/s) compared to As(III)-free conditions. This result confirms that the addition of As(III) promoted an increase in the molecular weight of ArsR-LuxR and ArsR$_{C34Y}$-LuxR.

https://doi.org/10.1021/acsomega.4c11704
ACS Omega 2025, 10, 14199−14208

CPM and diffusion coefficient values indicated that As(III)-promoted aggregates of these proteins may be included in the soluble cell lysates. In fact, both the whole fraction and the insoluble fraction, which contained these aggregates, exhibited significant noise, making accurate measurements by FCS difficult. Therefore, in this study, we conducted analyses using the supernatant (soluble) fraction obtained by centrifugation to remove these aggregates. Furthermore, even in the soluble fraction after centrifugation, FCS analysis detected components with significantly larger molecular sizes under As(III) treatment conditions compared to the monomer. This suggests that some level of aggregation also occurs within the soluble fraction. Since the aggregates were found in the soluble fraction after centrifugation, this strongly suggests that large aggregates with high molecular weights could be formed inside the cell. Therefore, As(III) may induce the aggregation of ArsR-LuxR and $ArsR_{C34Y}$-LuxR in the cells.

CONCLUSION

In this study, we developed a novel sensor system by engineering a single plasmid capable of expressing both LuxR, an As(III) aggregation-based sensor previously reported, and the intracellular As(III) metabolism regulator ArsR, for portable introduction into various *E. coli* strains. When expressed in the *E. coli* MG1655 strain, the super-repressor mutant $ArsR_{C34Y}$-LuxR suppressed the expression of the As(III) efflux protein ArsB, enabling the intracellular As(III) concentration to reach its upper limit even at an extracellular As(III) concentration of 13.35 μM, which is 1 order of magnitude lower than previously observed concentrations. This induced LuxR aggregation, successfully demonstrating the upper limit of As(III) uptake that *E. coli* cells can tolerate before exhibiting As(III) toxicity. Additionally, it was found that both ArsR-LuxR and $ArsR_{C34Y}$-LuxR formed aggregates in response to As(III), thereby switching the transcriptional activation function of LuxR. In our previous report, it was merely shown that LuxR forms precipitates in the insoluble fraction in the presence of As(III). However, the present study revealed that LuxR exists as aggregates within the soluble fraction. The $ArsR_{C34Y}$-LuxR sensor system provides a novel mechanism for highly sensitive detection of As(III), functioning as a trigger for LuxR aggregation that leads to a functional switch.

The behavior of this aggregation-based sensor parallels findings from Lindquist and colleagues, who demonstrated that protein aggregation can drive functional switches, as observed in their studies on yeast prions. Specifically, they reported that the yeast prion [*PSI*$^+$] generates phenotypic diversity through nonsense codon read-through, facilitating adaptation to environmental changes and promoting the evolution of new traits.[35] Notably, yeast prion Sup35 oligomers in the [*PSI*$^+$] yeast strain enable epigenetic phenotypic switches. This phenomenon is analogous to the LuxR aggregation observed in our study, where aggregation facilitates the functional switch of transcriptional activation.

However, unlike the amyloid oligomers of the yeast prion Sup35, the LuxR aggregation induced by As(III) is characterized by disordered, amorphous aggregation. Due to this nature, even when $ArsR_{C34Y}$ aggregates, it does not dissociate from the DNA operator sequence pArs. This observation suggests that the functional switching ability of $ArsR_{C34Y}$ may be lower than that of amyloid-based aggregation systems like Sup35.

Furthermore, as Lindquist and colleagues proposed that [*PSI*$^+$]-mediated epigenetic changes could contribute to evolutionary processes, our study suggests that the $ArsR_{C34Y}$-LuxR aggregation-based sensor may provide an adaptive mechanism, enabling cells to rapidly switch functions in response to As(III) concentrations. The insights gained from the aggregation-based sensor developed in this study extend beyond the development of microbial As(III) sensors, offering potential contributions to the understanding of intracellular functional switch mechanisms and their application in designing adaptive systems for environmental stress conditions.

MATERIAL AND METHODS

Bacterial Strains, Media, and Growth Conditions. *E. coli* strains MG1655 was used throughout this work, JW3469 and BW25113 were also used for analysis, and XL10-Gold (Kan) (Stratagene, La Jolla, CA) was used for cloning JW3469 stain was single-gene knockout mutant and it requested for distribution from NBRP *E. coli* strain. In all experiments, *E. coli* strains were incubated in LB medium (2.0% (w/v) LB Borth, Lennox, Nacalai Tesque, Kyoto, Japan) or on LB agar plates (2.0% (w/v) LB, 1.5% (w/v) agar; Nacalai Tesque) at 37 °C. Antibiotics were added in the following concentrations: 100 mg/mL of ampicillin (Nacalai Tesque) to maintain the pUC19 based vector and/or 30 mg/mL chloramphenicol (Nacalai Tesque) to maintain the pAC-based vector (pLux-sfgfp-HSVtk-aph, referred to as pLux-sfgfp[28,36]) and/or 20 mg/mL streptomycin (Nacalai Tesque) to maintain the pCDF-base vector (pArs-mCherry-SmR) and/or kanamycin (Nacalai Tesque) to maintain JW3469 strain30. The AHL (*N*-(3-oxohexanoyl)-L-homoserine lactone; acyl homoserine lactone) used in this study and was purchased from Sigma-Aldrich. This stock solution (10 mM) was prepared by dissolving appropriate amounts of the compounds in ethyl acetate (Nacalai Tesque) that was acidified with glacial acetic acid (0.01% (v/v); Nacalai Tesque) and was stored at −20 °C. The As(III) used in this study was Arsenic Standard Solution (As 1000 mg/L, composition: As_2O_3 and NaOH in water pH 5.0 with HCl, Fujifilm Wako Pure Chemical Corporation, Osaka, Japan).

Plasmid Construction. The LuxR reading frame fused with a histidine hexamer at the C-terminus was inserted into the *Xho*I/*BamH*I cleavage site of the pUC-based vector, controlled by the BBa_J23116 promoter from the Anderson promoter collection (http://parts.igem.org/Promoters/Catalog/Anderson), yielding pUC19-PJ23116-LuxR36. The ArsR-LuxR construct was generated by amplifying the full-length *arsR* gene sequence, excluding the stop codon, from the genome of *E. coli* MG1655 using primers containing *Xho*I and *Spe*I restriction enzyme sites at their ends. The *luxR* gene, excluding the start codon, was positioned downstream, and the two genes were joined using the *Spe*I restriction enzyme site as a linker sequence. The amplified *arsR* gene was cloned into the pUC19-PJ23116-LuxR plasmid. Using ArsR-LuxR as a template, the C34Y mutation was introduced into the *arsR* region to produce the $ArsR_{C34Y}$-LuxR construct.

Analysis of LuxR, ArsR-LuxR and $ArsR_{C34Y}$-LuxR Response to As(III) Using sfGFP and mCherry as the Reporter. For the quantitative assay, MG1655 harboring pLux-sfgfp, pArs-mCherry and LuxR, ArsR-LuxR or $ArsR_{C34Y}$-LuxR were first grown overnight from single colonies in LB medium. Then, 1% cultures were inoculated into 500 μL of LB medium that included appropriate antibiotics, 10 μM AHL and

https://doi.org/10.1021/acsomega.4c11704
ACS Omega 2025, 10, 14199−14208

varying concentrations of As(III) (0−133.5 μM) in 96-well deep-well plates. These cultures were shaken at 37 °C for 12 h. The 20 mL cultures were diluted 10-fold into saline (0.9% (w/v) NaCl; Nacalai Tesque) in 96 shallow-well plates. Cell density (OD_{600}) and fluorescence intensity (excitation: 485 nm, emission: 535 nm for sfGFP, excitation: 535 nm, emission: 615 nm for mCherry) were measured using FilterMax F5 (Molecular Devices, Sunnyvale, CA, USA) for Figures 1, 2 and S2. Cell density (OD_{600}) was measured on a Spectra Max (MOLECULAR DEVICE, San Jose, CA, USA), and fluorescence intensity (excitation: 485 nm, emission: 510 nm) was measured using Fluoroskan Ascent (Thermo Scientific, Waltham, MA, USA) for Figure 3. The GFP/mCherry ratio was calculated by dividing the fluorescence intensity of GFP by that of mCherry for each sample.

Determination of Arsenic Concentration. The resultant plasmids were introduced into MG1655 harboring pLux-sfgfp. The transformants were incubated overnight in 2 mL of LB medium. A 100 μL aliquot of the culture was added to 10 mL of fresh LB medium that included appropriate antibiotics, 10 μM AHL and varying concentrations of As(III) (0−133.5 μM), and incubated at 37 °C for 12 h with shaking. After the incubation, the cells at a concentration of 10^{10} were washed with and resuspended in 0.9% sodium chloride (99.999%, Sigma-Aldrich, St. Louis, MO) solution and centrifuged at 3000*g* for 5 min at 4 °C to collect the cell pellet. The cell pellet was incinerated with 200 μL of concentrated nitric acid (60%, Fujifilm Wako Pure Chemical Corporation) by heating on a hot plate, and then diluted with Milli-Q water (Millipore, Tokyo, Japan) for elemental analysis by using ICP−MS (Agilent 8800 ICP−MS/MS; Agilent Technologies, Tokyo, Japan). The signal intensity of arsenic was monitored at m/z 75 with an integration time of 0.1 s, and the arsenic concentration was calculated using a standard calibration method with yttrium (Y) monitored at m/z 89 as the internal standard.

Preparation for Cell Lysates. The resultant plasmids were introduced into MG1655 harboring pLux-sfgfp. The transformants were incubated overnight in 2 mL of LB medium. A 100 μL aliquot of the culture was added to 10 mL of fresh LB medium that included appropriate antibiotics, 10 μM AHL and varying concentrations of As(III) (0−133.5 μM), and shaken at 37 °C for 12 h. Subsequently, the cells were centrifuged at 3000*g* for 5 min at 4 °C to collect the resultant cell pellet. The cells were washed with wash buffer 20 mM HEPES, pH 7.6, 500 mM NaCl,10% (v/v) glycerol) and centrifuged at 3000*g* for 5 min at 4 °C. The cells were resuspended to a concentration of 10^{10} cells/mL in sonication lysis buffer (20 mM HEPES, pH 7.6, 500 mM NaCl,10% (v/v) glycerol, 0.1 mg/mL lysozyme, and supplemented with 1 tablet cOmplete Mini EDTA-free Protease Inhibitor Cocktail per 10 mL (Roche Diagnostics, Mannheim, Germany)). The cell suspension was sonicated for 10 min at 4 °C or below (QSONICA, Amplitude 40, Process Time 20 min (Pulse-ON 2 s, Pulse-OFF 7 s) .

Western Blot Analysis of Sensor Proteins. A histidine hexamer was fused in frame to the C-terminus of the reading frames of sensor proteins. The lysate was rigorously centrifuged (20,817*g* for 30 min at 4 °C), and the supernatant was taken as a soluble fraction. The total and soluble fraction thus obtained was diluted with 2× SDS sample buffer (0.1 M Tris, pH 6.8, 4% (w/v) SDS, 20% (v/v) glycerol, 12% (v/v) mercaptoethanol, and 0.036% (w/v) bromophenol blue), and boiled for 5 min. Total 20 μg protein obtained from each sample was loaded on an acrylamide gel (10% (w/v)). The protein in the gel was then transferred to a PVDF membrane for 1 h at 100 mA. The membrane was incubated for 1 h in TBS-T (20 mM Tris HCl, 0.8% NaCl, and 0.2% Tween 20) containing 5% skim milk and washed 3 times with TBS-T solution. The membrane was incubated for 1 h in 4 mL of TBS-T containing 5% skim milk with 0.1% (v/v) 6His mAb-HRP Conjugate (Clontech, Takara Bio, Shiga, Japan) at room temperature. The membrane was then washed three times in TBS-T. Finally, the bound antibody was detected using chemiluminescence (ImmunoStar LD, Fujifilm Wako Pure Chemical Corporation).

Fluorescence Correlation Spectroscopy Analysis. Fluorescence correlation spectroscopy measurements were performed using an LSM 510 META + ConfoCor 3 system with a C-Apochromat 40 × 1.2NA Korr. UV−vis-IR water immersion objective (Carl Zeiss, Jena, Germany),[31,37] The confocal pinhole diameter was adjusted to 66 μm. Emission signals were detected using avalanche photodiodes through a beam splitter 405/488 nm (HFT405/288) and a 505−610 nm band-pass filter. Each cell lysate was rigorously centrifuged (20,817*g* for 25 min at 4 °C), and the supernatant was recovered as a soluble fraction. Fluorescence signals of the samples were recorded on Lab-Tek 8-well chamber slides (Thermo Fisher) at 25 °C. As a control that does not respond to As(III), the soluble fraction of lysate from *E. coli* expressing sfGFP monomers. Curve fitting analysis for acquired autocorrelation function was performed using ZEN 2.3 SP1 software (Carl Zeiss) using a model for multiple components of 3D diffusion with a one-component exponential decay as the following eq 1

$$G(\tau) = 1 + \left[1 + \frac{T}{1-T}\exp\left(-\frac{\tau}{\tau_T}\right)\right]\frac{1}{N}\left[\sum_i^m F_i\left(1+\frac{\tau}{\tau_i}\right)^{-1}\left(1+\frac{\tau}{s^2\tau_i}\right)^{-1/2}\right] \quad (1)$$

where $G(\tau)$ is a fluorescence autocorrelation function from which the time (τ); F_i and τ_i are the fraction and diffusion time of 3D diffusion component i, respectively; N is the average number of fluorescent molecules in the detection confocal volume defined by the beam waist w_0 and the axial radius z_0; s is the structure parameter representing the ratio of w_0 to z_0; m is the number of components (m = 1 or 2); T is the exponential decay fraction; and τ_T is the relaxation time of the exponential decay. After adjustment of pinhole positions, the diffusion time and structure parameter were determined using an ATTO488 solution as a standard fluorescent dye. $G(\tau)$ of the samples in aqueous solutions were acquired for 300 s. The diffusion coefficient of the samples was calculated based on that of ATTO488 in solution and its diffusion coefficient (400 $\mu m^2/s$). CPM was calculated as the mean photon count rates were divided by N. The represented CPM values of the samples were normalized to those of sfGFP monomers. Regarding the diffusion coefficients, a single-component analysis was performed for sfGFP monomers, while a two-component analysis was conducted for other samples, followed by the calculation of the weighted average.

https://doi.org/10.1021/acsomega.4c11704
ACS Omega 2025, 10, 14199−14208

■ ASSOCIATED CONTENT

Supporting Information

The Supporting Information is available free of charge at https://pubs.acs.org/doi/10.1021/acsomega.4c11704.

Figure S1. As(III) dose-responsive OD_{600}. The strain expressing the LuxR sensor in MG1655 is shown with black circles, the strain expressing the LuxR sensor in JW3469 is shown with yellow circles, and the MG1655 strain expressing only the vector is shown with gray circles. Each plot represents the average of three independent experiments, and error bars represent standard deviations. Figure S2 Response of ArsR-LuxR and $ArsR_{C34Y}$-LuxR sensors to As(III) in BW25113 strain. Upper: dose-dependent response to As(III) of ArsR-LuxR (red circles) or $ArsR_{C34Y}$-LuxR (blue circles) in BW25113 strains were analyzed. Each strain was cotransformed with the reporter plasmids pLux-sfgfp to evaluate the As(III)-dependent transcriptional activation by LuxR. Each plot represents the average of three independent experiments, and error bars indicate standard deviations. Lower: OD_{600} dose-responsive changes to As(III). * indicates the point at which growth inhibition in $ArsR_{C34Y}$-LuxR strain. Each plot represents the average of three independent experiments, and error bars indicate standard deviations (PDF)

■ AUTHOR INFORMATION

Corresponding Author

Shigeko Kawai-Noma − *Department of Applied Chemistry and Biotechnology, Chiba University, Chiba 263-8522, Japan;* orcid.org/0000-0002-4753-7652; Phone: +81-43-290-3391; Email: kawai-noma@chiba-u.jp; Fax: +81-43-290-3413

Authors

Shiryu Abe − *Department of Applied Chemistry and Biotechnology, Chiba University, Chiba 263-8522, Japan*

Rina Ayuba − *Department of Applied Chemistry and Biotechnology, Chiba University, Chiba 263-8522, Japan*

Kyohei Ouchi − *Department of Applied Chemistry and Biotechnology, Chiba University, Chiba 263-8522, Japan*

Yu-ki Tanaka − *Graduate School of Pharmaceutical Sciences, Chiba University, Chiba 260-8675, Japan;* orcid.org/0000-0001-8298-7408

Ai Fujimoto − *Faculty of Advanced Life Science, Hokkaido University, Sapporo 001-0021, Japan;* orcid.org/0000-0003-3572-4001

Akira Kitamura − *Faculty of Advanced Life Science, Hokkaido University, Sapporo 001-0021, Japan;* orcid.org/0000-0001-8357-8593

Yasumitsu Ogra − *Graduate School of Pharmaceutical Sciences, Chiba University, Chiba 260-8675, Japan;* orcid.org/0000-0002-8268-1828

Yuki Kimura − *Department of Applied Chemistry, Waseda University, Tokyo 169-8555, Japan;* orcid.org/0000-0002-1011-3485

Daisuke Umeno − *Department of Applied Chemistry, Waseda University, Tokyo 169-8555, Japan;* orcid.org/0000-0001-8107-552X

Complete contact information is available at: https://pubs.acs.org/10.1021/acsomega.4c11704

Author Contributions

⊥S.A. and R.A. are equally contributed. All authors designed the research. S.A., R.A., and K.O. performed all experiments with assistance from Y.K., D.U., and S.K.-N. Y.T. and Y.O. performed ICP−MS. A.F. and A.K. performed FCS. S.A., Y.T., A.K., D.U., and S.K.-N. wrote the manuscript.

Notes

The authors declare no competing financial interest.

All data are presented as mean ± standard error from at least three independent trials. Statistical significance was determined using Student's *t* tests performed with Microsoft Excel.

■ ACKNOWLEDGMENTS

This work was supported by The Hamaguchi Foundation for the Advancement of Biochemistry and Yamada Science Foundation. D.U. conducted this work as a part of Waseda Research Institute for Science and Engineering project "Experimental Evolution of Genetic Devices (22P04), supported by JSPS Kakenhi Grants 16H06450, 18H01791, 21H01721 and by the Salt Science Research Foundation (no.2404).

■ ABBREVIATIONS

AHL, *N*-(3-oxohexanoyl)-L-homoserine lactone; acyl homoserine lactone; Amp, ampicillin; *ars*, arsenic resistance; As(III), arsenite; *Cm*, chloramphenicol; CPM, counts per molecule; FCS, fluorescence correlation spectroscopy; GFP, green fluorescent protein; ICP−MS, inductively coupled plasma mass spectrometry; sfGFP, superfolder green fluorescent protein

■ REFERENCES

(1) Ravenscroft, P. *Predicting the Global Extent of Arsenic Pollution of Groundwater and its Potential Impact on Human Health*; UNICEF, 2007.

(2) Ng, J.; Gomez-Caminero, A. *Arsenic and Arsenic Compounds*, 2nd ed.; World Health Organization: Geneva, 2001.

(3) Takeuchi, A.; Namera, A.; Kawasumi, Y.; Imanaka, T.; Sakui, N.; Ota, H.; Endo, Y.; Sumino, K.; Endo, G. Development of an Analytical Method for the Determination of Arsenic in Urine by Gas Chromatography-mass Spectrometry for Biological Monitoring of Exposure to Inorganic Arsenic. *J. Occup. Health* **2012**, *54* (6), 434−440.

(4) Klaue, B.; Blum, J. D. Trace Analyses of Arsenic in Drinking Water by Inductively Coupled Plasma Mass Spectrometry: High Resolution versus Hydride Generation. *Anal. Chem.* **1999**, *71* (7), 1408−1414.

(5) Melamed, D. Monitoring Arsenic in the Environment: A Review of Science and Technologies with the Potential for Field Measurements. *Anal. Chim. Acta* **2005**, *532* (1), 1−13.

(6) Li, H.; Liang, C.; Chen, W.; Jin, J.-M.; Tang, S.-Y.; Tao, Y. Monitoring in Vivo Metabolic Flux with a Designed Whole-Cell Metabolite Biosensor of Shikimic Acid. *Biosens. Bioelectron.* **2017**, *98*, 457−465.

(7) Wang, B.; Barahona, M.; Buck, M. A Modular Cell-Based Biosensor Using Engineered Genetic Logic Circuits to Detect and Integrate Multiple Environmental Signals. *Biosens. Bioelectron.* **2013**, *40* (1), 368−376.

(8) Hanko, E. K. R.; Minton, N. P.; Malys, N. A Transcription Factor-Based Biosensor for Detection of Itaconic Acid. *ACS Synth. Biol.* **2018**, *7* (5), 1436−1446.

(9) Kim, H. J.; Lim, J. W.; Jeong, H.; Lee, S.-J.; Lee, D.-W.; Kim, T.; Lee, S. J. Development of a Highly Specific and Sensitive Cadmium and Lead Microbial Biosensor Using Synthetic CadC-T7 Genetic Circuitry. *Biosens. Bioelectron.* **2016**, *79*, 701−708.

(10) Kim, H. J.; Jeong, H.; Lee, S. J. Synthetic Biology for Microbial Heavy Metal Biosensors. *Anal. Bioanal. Chem.* **2018**, *410* (4), 1191−1203.
(11) Van Der Meer, J. R.; Belkin, S. Where Microbiology Meets Microengineering: Design and Applications of Reporter Bacteria. *Nat. Rev. Microbiol.* **2010**, *8* (7), 511−522.
(12) Ordóñez, E.; Thiyagarajan, S.; Cook, J. D.; Stemmler, T. L.; Gil, J. A.; Mateos, L. M.; Rosen, B. P. Evolution of Metal(Loid) Binding Sites in Transcriptional Regulators. *J. Biol. Chem.* **2008**, *283* (37), 25706−25714.
(13) Shi, W.; Dong, J.; Scott, R. A.; Ksenzenko, M. Y.; Rosen, B. P. The Role of Arsenic-Thiol Interactions in Metalloregulation of the Ars Operon. *J. Biol. Chem.* **1996**, *271* (16), 9291−9297.
(14) Xu, C.; Zhou, T.; Kuroda, M.; Rosen, B. P. Metalloid Resistance Mechanisms in Prokaryotes. *J. Biochem.* **1998**, *123* (1), 16−23.
(15) Chen, S.-Y.; Wei, W.; Yin, B.-C.; Tong, Y.; Lu, J.; Ye, B.-C. Development of a Highly Sensitive Whole-Cell Biosensor for Arsenite Detection through Engineered Promoter Modifications. *ACS Synth. Biol.* **2019**, *8* (10), 2295−2302.
(16) Ramanathan, S.; Shi, W.; Rosen, B. P.; Daunert, S. Bacteria-Based Chemiluminescence Sensing System Using β-Galactosidase under the Control of the ArsR Regulatory Protein of the Ars Operon. *Anal. Chim. Acta* **1998**, *369*, 189−195.
(17) Roberto, F. Evaluation of a GFP Reporter Gene Construct for Environmental Arsenic Detection. *Talanta* **2002**, *58* (1), 181−188.
(18) Stocker, J.; Balluch, D.; Gsell, M.; Harms, H.; Feliciano, J.; Daunert, S.; Malik, K. A.; Van Der Meer, J. R. Development of a Set of Simple Bacterial Biosensors for Quantitative and Rapid Measurements of Arsenite and Arsenate in Potable Water. *Environ. Sci. Technol.* **2003**, *37* (20), 4743−4750.
(19) Tani, C.; Inoue, K.; Tani, Y.; Harun-ur-Rashid, Md.; Azuma, N.; Ueda, S.; Yoshida, K.; Maeda, I. Sensitive Fluorescent Microplate Bioassay Using Recombinant Escherichia Coli with Multiple Promoter−Reporter Units in Tandem for Detection of Arsenic. *J. Biosci. Bioeng.* **2009**, *108* (5), 414−420.
(20) Wan, X.; Volpetti, F.; Petrova, E.; French, C.; Maerkl, S. J.; Wang, B. Cascaded Amplifying Circuits Enable Ultrasensitive Cellular Sensors for Toxic Metals. *Nat. Chem. Biol.* **2019**, *15* (5), 540−548.
(21) Shen, S.; Li, X.-F.; Cullen, W. R.; Weinfeld, M.; Le, X. C. Arsenic Binding to Proteins. *Chem. Rev.* **2013**, *113* (10), 7769−7792.
(22) Kitchin, K. T.; Wallace, K.; Andrewes, P. Some Chemical Properties Underlying Arsenic's Biological Activityp. *Proceedings of the Fifth International Conference on Arsenic Exposure and Health Effects*, 2002.
(23) Shi, W.; Wu, J.; Rosen, B. P. Identification of a Putative Metal Binding Site in a New Family of Metalloregulatory Proteins. *J. Biol. Chem.* **1994**, *269* (31), 19826−19829.
(24) Xu, C.; Rosen, B. P. Dimerization Is Essential for DNA Binding and Repression by the ArsR Metalloregulatory Protein of Escherichia Coli. *J. Biol. Chem.* **1997**, *272* (25), 15734−15738.
(25) Stevens, A. M.; Queneau, Y.; Soulère, L.; Bodman, S. V.; Doutheau, A. Mechanisms and Synthetic Modulators of AHL-Dependent Gene Regulation. *Chem. Rev.* **2011**, *111* (1), 4−27.
(26) Fuqua, W. C.; Winans, S. C.; Greenberg, E. P. Quorum Sensing in Bacteria: The LuxR-LuxI Family of Cell Density-Responsive Transcriptional Regulators. *J. Bacteriol.* **1994**, *176* (2), 269−275.
(27) Ng, W.-L.; Bassler, B. L. Bacterial Quorum-Sensing Network Architectures. *Annu. Rev. Genet.* **2009**, *43* (1), 197−222.
(28) Ayuba, R.; Umeno, D.; Kawai-Noma, S. OFF-Switching Property of Quorum Sensor LuxR via As(III)-Induced Insoluble Form. *J. Biosci. Bioeng.* **2022**, *133* (4), 335−339.
(29) Meng, Y.-L.; Liu, Z.; Rosen, B. P. As(III) and Sb(III) Uptake by GlpF and Efflux by ArsB in Escherichia Coli. *J. Biol. Chem.* **2004**, *279* (18), 18334−18341.
(30) Baba, T.; Ara, T.; Hasegawa, M.; Takai, Y.; Okumura, Y.; Baba, M.; Datsenko, K. A.; Tomita, M.; Wanner, B. L.; Mori, H. Construction of Escherichia Coli K-12 In-frame, Single-gene Knockout Mutants: The Keio Collection. *Mol. Syst. Biol.* **2006**, *2* (1), 2006-0008.
(31) Kitamura, A.; Fujimoto, A.; Kawashima, R.; Lyu, Y.; Sasaki, K.; Hamada, Y.; Moriya, K.; Kurata, A.; Takahashi, K.; Brielmann, R.; Bott, L. C.; Morimoto, R. I.; Kinjo, M. Hetero-Oligomerization of TDP-43 Carboxy-Terminal Fragments with Cellular Proteins Contributes to Proteotoxicity. *Commun. Biol.* **2024**, *7* (1), 743.
(32) Kawai-Noma, S.; Ayano, S.; Pack, C.; Kinjo, M.; Yoshida, M.; Yasuda, K.; Taguchi, H. Dynamics of Yeast Prion Aggregates in Single Living Cells. *Genes Cells* **2006**, *11* (9), 1085−1096.
(33) Kawai-Noma, S.; Pack, C.; Tsuji, T.; Kinjo, M.; Taguchi, H. Single Mother−Daughter Pair Analysis to Clarify the Diffusion Properties of Yeast Prion Sup35 in guanidine-HCl-treated [PSI$^+$] Cells. *Genes Cells* **2009**, *14* (9), 1045−1054.
(34) Kawai-Noma, S.; Pack, C.-G.; Kojidani, T.; Asakawa, H.; Hiraoka, Y.; Kinjo, M.; Haraguchi, T.; Taguchi, H.; Hirata, A. In Vivo Evidence for the Fibrillar Structures of Sup35 Prions in Yeast Cells. *J. Cell Biol.* **2010**, *190* (2), 223−231.
(35) True, H. L.; Lindquist, S. L. A Yeast Prion Provides a Mechanism for Genetic Variation and Phenotypic Diversity. *Nature* **2000**, *407* (6803), 477−483.
(36) Kimura, Y.; Kawai-Noma, S.; Saito, K.; Umeno, D. Directed Evolution of the Stringency of the LuxR Vibrio Fischeri Quorum Sensor without OFF-State Selection. *ACS Synth. Biol.* **2020**, *9* (3), 567−575.
(37) Kitamura, A.; Nakayama, Y.; Shibasaki, A.; Taki, A.; Yuno, S.; Takeda, K.; Yahara, M.; Tanabe, N.; Kinjo, M. Interaction of RNA with a C-Terminal Fragment of the Amyotrophic Lateral Sclerosis-Associated TDP43 Reduces Cytotoxicity. *Sci. Rep.* **2016**, *6* (1), 19230.

https://doi.org/10.1021/acsomega.4c11704
ACS Omega 2025, 10, 14199−14208